Spherical deca-vanadophosphate covalent assembled all-inorganic open framework

Hailiang Hu, Zhenyu Guo, Kaixuan Li, Xiaoling Lin, Yang Liu,* and Zhenhui Kang*

Supporting Information

Experimental

Materials and Measurements.

All materials were reagent grade obtained from commercial sources and used without further purification. IR spectrum was recorded in the range 4000-400 cm^{-1} on a HYPERION spectrometer with a pressed KBr pellet. UV-Vis absorption was recorded on a Lambda 750 (Perking Elmer) spectrophotometer in the wavelength range of 300-800 nm at room temperature. The thermogravimetric analysis (TGA) was carried out by Universal Analysis 2000 TG analyzer in N_2 and air with a heating rate of 10 °C /min, respectively. Powder X-ray diffraction (XRD) data were collected on an X'Pert-ProMPD (Holand) D/max-γA X-ray diffractometer with Cu Kα radiation in a flat plate geometry. The gas-sorption experiments (up to 1 atm) were performed on ASAP 2020 and 2050 Xtended Pressure Sorption Analyzer. Scanning electron microscopy (SEM) and Energy-dispersive X-ray (EDX) analysis were performed on a FEI/Philips Tecnai 12 BioTWIN transmission electron micro-scope. The X-ray Photoelectron Spectroscopy (XPS) spectra were obtained with a KRATOS Axis ultra DLD X-ray photoelectron spectrometer with a monochromatised Mg Kα X-55 ray (hν = 1283.3 eV). XPS samples were prepared by pressing the powder material into an indium support. Electrochemical measurements were performed with a CHI 660E workstation (CH Instruments, Chenhua, Shanghai, China). All electrochemical experiments were

carried out at room temperature. The electrocatalytic activity of **1** was tested in a conventional three-electrode cell. A saturated calomel electrode Ag/AgCl was used as a reference electrode (SCE), and a Pt wire was used as a counter electrode. Chemically bulk-modified carbon paste electrode (CPE) was used as the working electrode. Mott-Schottky plot was performed within the potential region of -0.50 to 1.2 V. An amplitude of 20 mV was applied, and the measured frequency was 1 kHz.

Theoretical methods

Optimized geometry was achieved using the B3LYP functional and LANL2DZ basis set for all complexes studied in this work. All calculations were performed using the Gaussian 09 package.

Synthesis.

A mixture of NH_4VO_3 (1.7 mmol), NaH_2PO_4 (0.5 mmol) and dmmt (0.46 mmol) was dissolved in 10.0 mL of distilled water and stirred briefly for 1.0 h. When the pH value was adjusted to about 8.7 with 1,4-butanediamine, the mixture was sealed into a 15 mL Teflon-lined autoclave and kept under autogenous pressure at 160 °C for 3 days. After cooling to room temperature slowly, black cubic crystals of **1** were filtered and washed with distilled water. (Yield about 35% based on V). IR (KBr pellet, cm^{-1}): 3440 (s), 1629 (m), 1401 (s), 1009 (s), 617 (m), 538 (w).

Preparations of 1-CPE.

Compound **1** modified carbon paste electrode (1-CPE) was fabricated as follows: 90 mg of graphite powder and 8 mg of compound **1** were mixed and ground together by an agate mortar and pestle to achieve a uniform mixture, and then 0.1 mL of Nujol was added with stirring. The homogenized mixture was packed into a glass tube with a 3.0 mm inner diameter, and the tube surface was wiped with weighing paper. Electrical contact was established with a copper rod through the back of the electrode.

X-ray Crystallographic Study.

Crystal data for compound **1** were collected on a Bruker APEX-II CCD diffractometer with Mo Kα radiation (λ = 0.71073 Å). The structures were solved by the direct methods and refined by full-matrix least-squares on F^2 using the *SHELXTL* crystallographic software package.[1] All non-hydrogen atoms were refined anisotropically. Hydrogen atoms attached to water molecule of O2W can't be generated and were included in the molecular formula directly. CCDC number is 1486615 for compound **1**.

Crystal data for **1**: $H_{42}N_9O_{54}P_6V_{15}$, M = 1982.34, black crystal, Cubic, space group *Im*-3*m*, a = 16.0271(5) Å, β = 90°, V = 4116.8(4) Å^3, Z = 2, T = 298 K, ρ_c = 1.599 g·cm^{-3}, μ = 1.818 mm^{-1}, R_1 [I > 2σ(I)] = 0.0842, wR_2 [all data] = 0.2560, GOF = 1.164.

Reference

1 (a) G. M. Sheldrick, *SHELXS-97, Program for solution of crystal structures,* University of GÖttingen, Germany, 1997; (b) G. M. Sheldrick, *SHELXL-97, Program for refinement of crystal structures*, University of Göttingen, Germany, 1997.

Table S1 Selected Bond lengths (Å) and angles (°) by X-ray and DFT calculations.

Bond Lengths	Exp.	Cal.	Bond Angles	Exp.	Cal.
P(1)-O(4)$^{\#9}$	1.532(5)	1.77972	O(4)$^{\#9}$-P(1)-O(4)$^{\#10}$	110.3(4)	109.79631
P(1)-O(4)$^{\#10}$	1.532(5)	1.61165	O(4)$^{\#9}$-P(1)-O(4)	109.07(18)	97.00669
P(1)-O(4)	1.532(5)	1.61165	O(4)$^{\#10}$-P(1)-O(4)	109.07(18)	109.79631
P(1)-O(4)$^{\#11}$	1.532(5)	1.77972	O(4)$^{\#9}$-P(1)-O(4)$^{\#11}$	109.07(18)	109.79631
V(1)-O(1)	1.61(2)	1.63210	O(4)$^{\#10}$-P(1)-O(4)$^{\#11}$	109.07(18)	118.51878
V(1)-O(2)$^{\#1}$	1.931(9)	1.88940	O(4)-P(1)-O(4)$^{\#11}$	109.07(18)	109.79631
V(1)-O(2)	1.931(9)	2.03217	O(1)-V(1)-O(2)$^{\#1}$	111.6(3)	115.96426
V(1)-O(2)$^{\#2}$	1.931(9)	1.88940	O(1)-V(1)-O(2)	111.6(3)	115.96426
V(1)-O(2)$^{\#3}$	1.931(9)	2.03217	O(2)$^{\#1}$-V(1)-O(2)	82.2(2)	81.11140
V(2)-O(3)$^{\#6}$	1.600(11)	1.61609	O(1)-V(1)-O(2)$^{\#2}$	111.6(3)	115.96426
V(2)-O(3)	1.600(11)	1.61609	O(2)$^{\#1}$-V(1)-O(2)$^{\#2}$	136.6(6)	138.66748
V(2)-O(2)$^{\#1}$	1.931(9)	1.88087	O(2)-V(1)-O(2)$^{\#2}$	79.5(12)	81.11098
V(2)-O(2)	1.931(9)	2.00617	O(1)-V(1)-O(2)$^{\#3}$	111.6(3)	115.96426
V(2)-O(4)	2.031(4)	2.01567	O(2)$^{\#1}$-V(1)-O(2)$^{\#3}$	82.2(2)	81.11098
Bond Angles	Exp.	Cal.	Bond Angles	Exp.	Cal.
O(2)-V(1)-O(2)$^{\#3}$	136.7(6)	128.07016	O(2)$^{\#1}$-V(2)-O(2)	80.8(5)	81.11140
O(2)$^{\#2}$-V(1)-O(2)$^{\#3}$	84.9(12)	83.83424	O(2)-V(2)-O(4)	146.9(4)	138.12693
O(2)$^{\#1}$-V(2)-O(4)$^{\#7}$	147.7(4)	138.12693	O(3)-V(2)-O(4)	112.3(12)	111.29556
O(3)$^{\#6}$-V(2)-O(2)	108.3(13)	111.29556	O(4)-V(2)-O(4)$^{\#7}$	81.5(2)	81.11140

Symmetry transformations used to generate equivalent atoms: #1 x, -z+2, y; #2 x, -z+2, -y+2; #3 x, -y+2, -z+2; #4 x, -y+2, z; #5 x, y, -z+2; #6 x, z, y; #7 -x+1, z, y; #9 y-1/2, -x+3/2, -z+3/2; #10 -x+1, -y+2, z; #11 -y+3/2, x+1/2, -z+3/2.

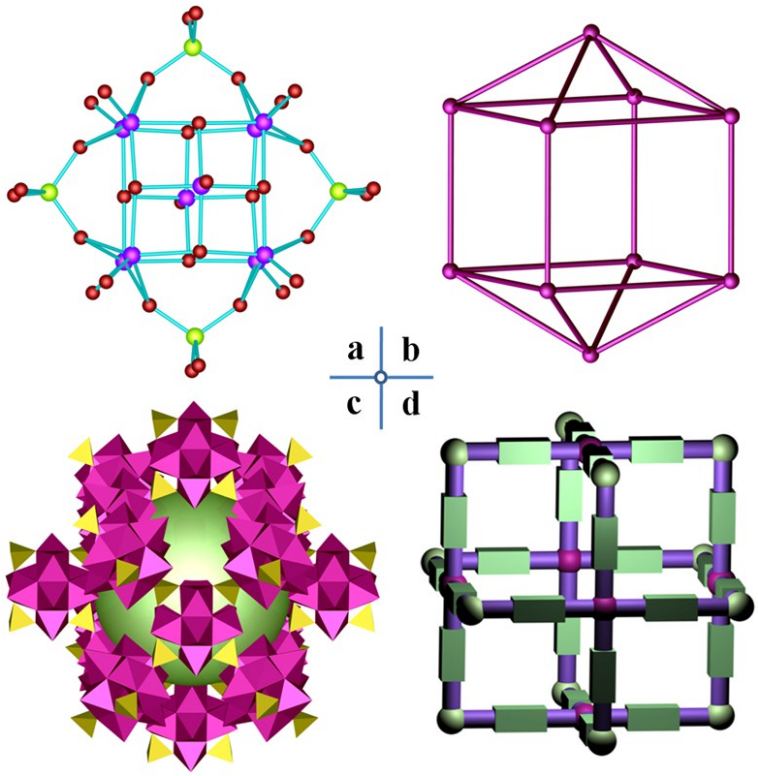

Fig. S1 Ball and stick representation of spherical hollow $\{P_4V_{10}\}$ cluster (a), and the $\{V_{10}\}$ dodecahedron (b). Nanosized $\{(P_4V_{10})_{18}\}$ cage (c). Perspective view of the truncated cuboctahedral cube (d).

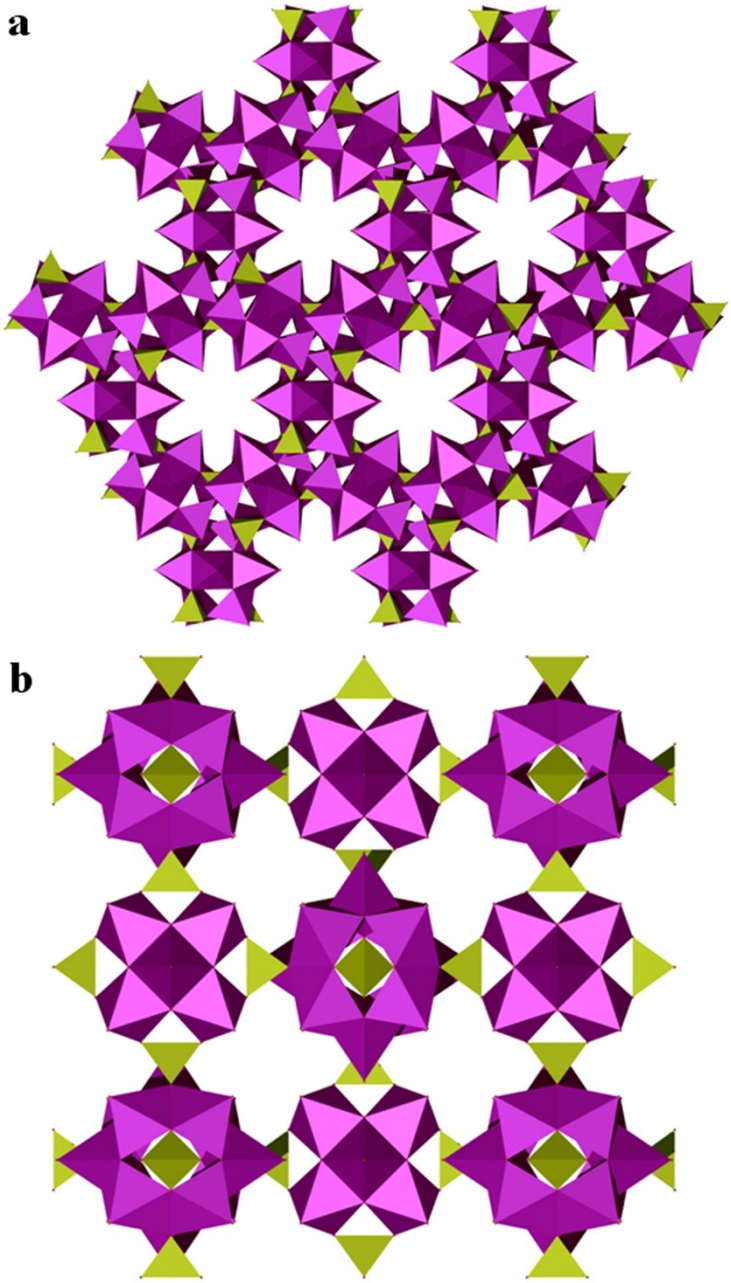

Fig. S2 Channel system of **1** that view along [111] direction (a), and [100] direction (b).

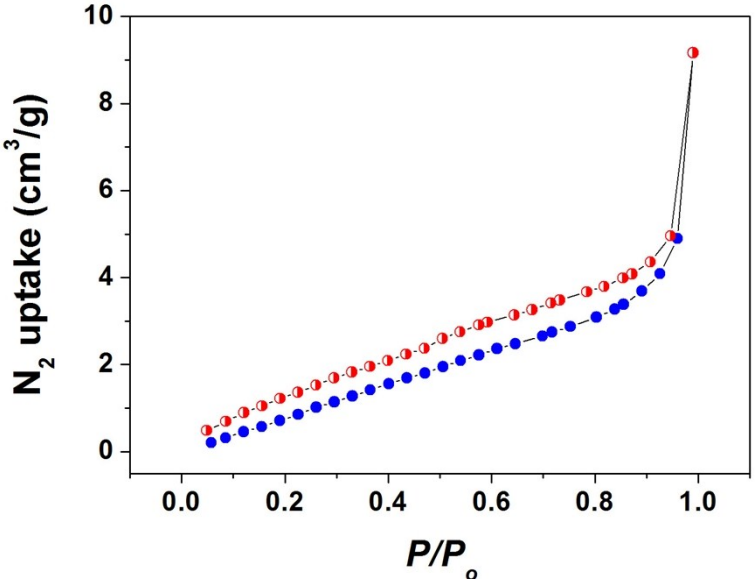

Fig. S3 N_2 adsorption–desorption isotherms measured at 77 K for compound **1**.

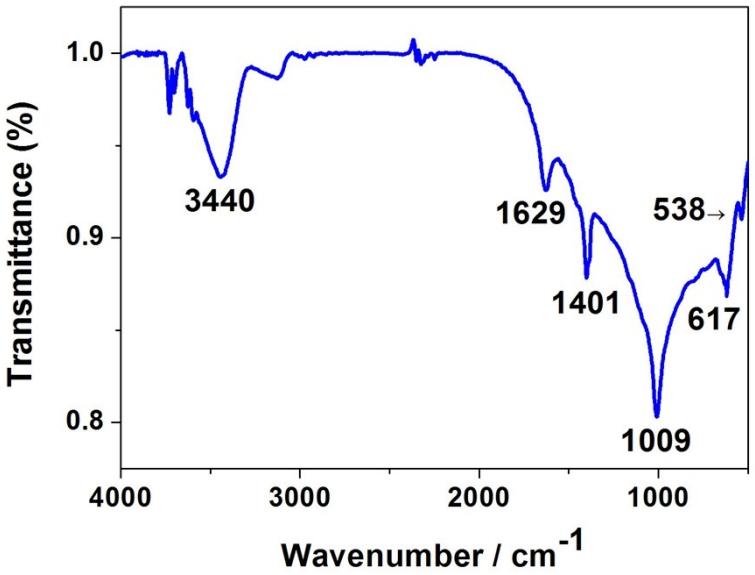

Fig. S4 FT-IR spectrum of compound **1**.

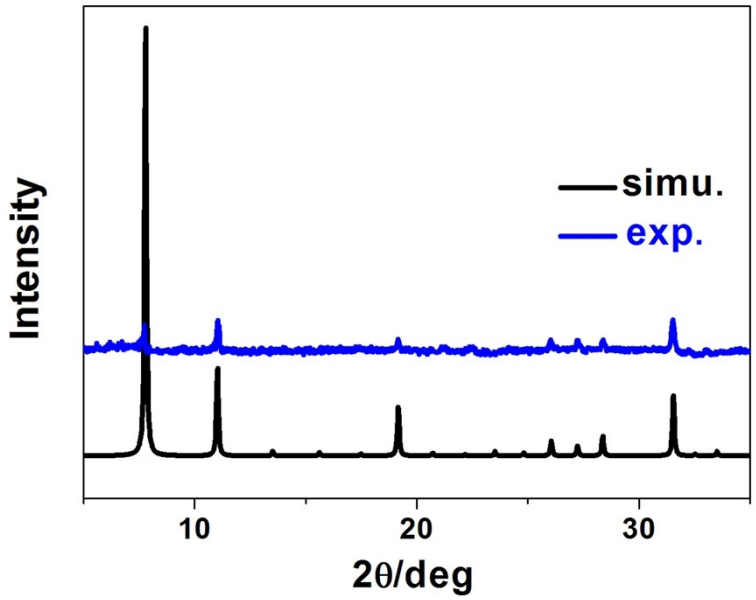

Fig. S5 Simulated and experimental XRD patterns of compound **1**. The diffraction peaks match well, indicating the good phase purity.

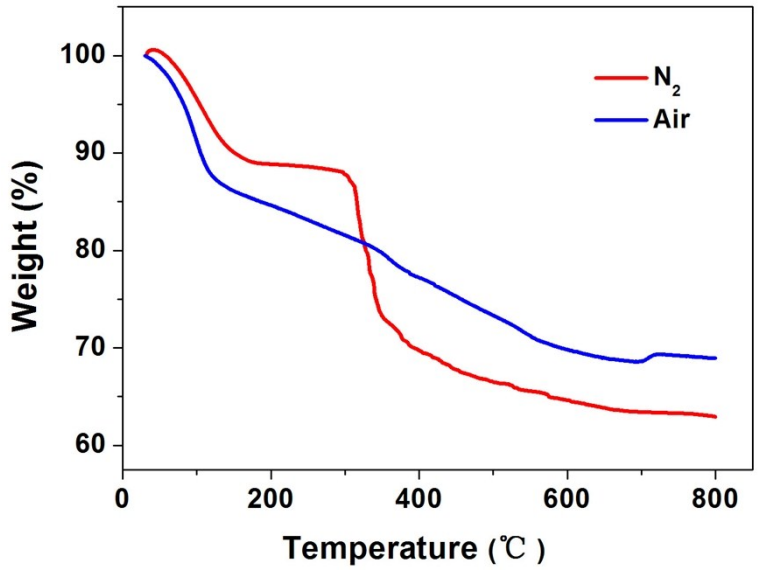

Fig. S6 TG curves of compound **1**. TG analysis was carried out with a heating rate of 10 °C/min under air and nitrogen flows, respectively.

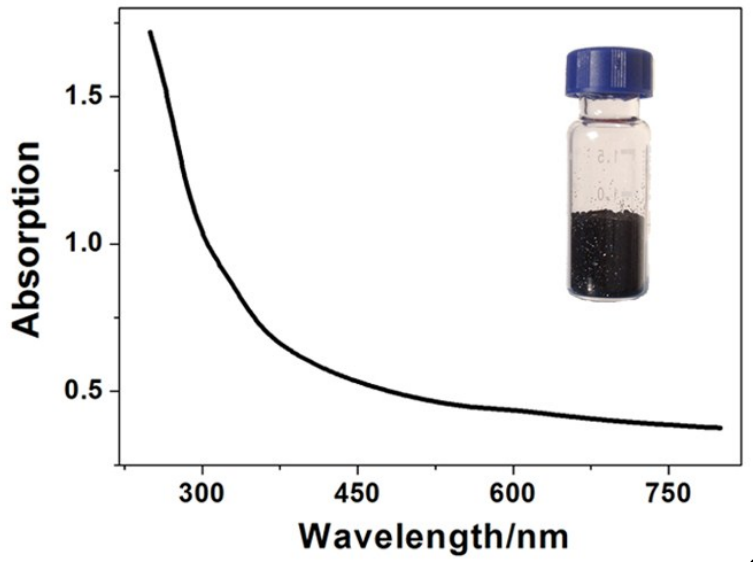

Fig. S7 The UV-vis spectrum and photograph image of black crystals **1**.

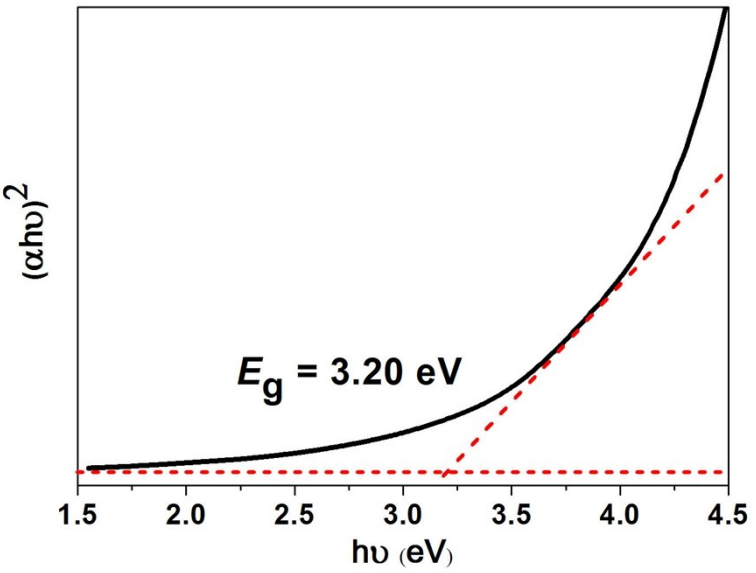

Fig. S8 The $(\alpha h\upsilon)^2$ vs. $h\upsilon$ curve of compound **1**. The dashed red lines mark the baseline and the tangent of the curve. When using r = 2, no good linear fit is obtained, and the band gap is estimated over 3.0 eV (intersection value).

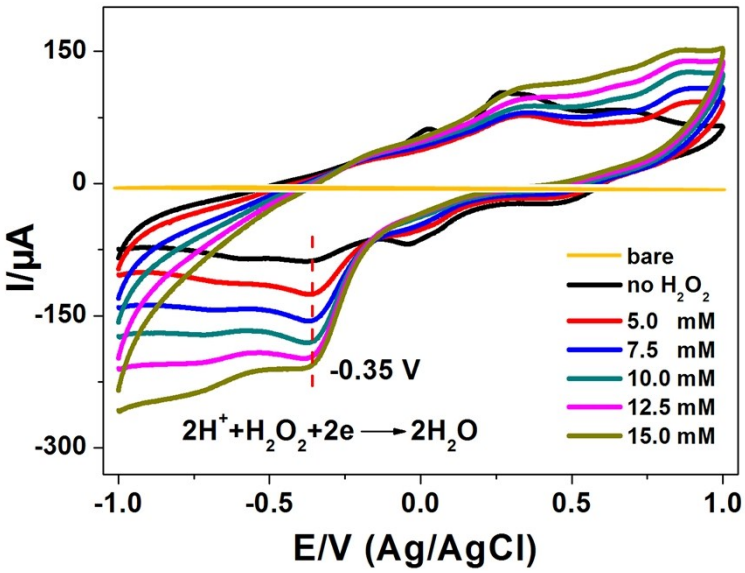

Fig. S9 CV curves of compound **1** in the presence of H_2O_2 with different concentrations (scan rate: 20 mv s^{-1}).